European Journal of Chemistry 2 (3) (2011) 394-403

European Journal of Chemistry

Journal homepage: www.eurjchem.com

Synthesis, characterization, antioxidant, antimicrobial, DNA binding and cleavage studies of mononuclear Cu(II) and Co(II) complexes of 3-hydroxy-*N*'-(2-hydroxybenzylidene)-2-naphthohydrazide

Linganna Shiva Kumar, Kollur Shiva Prasad and Hosakere Doddarevanna Revanasiddappa*

Department of Chemistry, University of Mysore, Manasagangotri, Mysore-570006, Karnataka, India

**Corresponding author at: Department of Chemistry, University of Mysore, Manasagangotri, Mysore-570006, Karnataka, India. Tel.: +91.821.2419669; fax: +91.821.2419363. E-mail address: hdrevanasiddappa@yahoo.com (H.D. Revanasiddappa).*

ARTICLE INFORMATION

Received: 06 August 2010
Received in revised form: 19 January 2011
Accepted: 17 February 2011
Online: 30 September 2011

KEYWORDS

Naphthohydrazide
Metal complexes
DNA binding
Oxidative cleavage
Antioxidant
Antimicrobial activity

ABSTRACT

In this report, we explore the DNA binding properties of mixed ligand copper(II)/cobalt(II) complexes of the type [M(bnp)(phen)H_2O].nH_2O, and copper(II)/cobalt(II) complexes of the type [M(Hbnp)$_2$], where n=0, 1, ..., H_2bnp=3-hydroxy-*N*'-(2-hydroxybenzylidene)-2-naphthohydrazide and phen=1,10-phenanthroline. A host of physical methods like spectral absorption, emission studies and hydrodynamic measurements have been used to probe the effect of ligands on the mode and extent of interaction of the complexes with Calf Thymus DNA. The efficiencies of the complexes to oxidatively cleaved pUC19 DNA was performed in the absence and presence of H_2O_2. Among the compounds tested for antioxidant capacity, H_2bnp displayed excellent activity than its complexes and standards used. It has been observed that Cu(II) and Co(II) complexes exhibited different levels of antibacterial and antifungal effects, with the assays carried out on four pathogenic bacteria and two pathogenic fungi. H_2bnp showed moderate activity against bacteria *E. coli*, *X. vesicatoria* and fungi, *A. niger* and *A. flavus*, but less than its complexes and standard drugs used for assay.

1. Introduction

The interest in the study of Schiff bases and their first-row transition metal complexes (such as Co(II), Cu(II) etc.) arises from their significant antimicrobial, antiviral, antitubercular and anticancer activities [1-4]. Hydrazones and molecules having hydrazide residues in their structures are capable of showing antifungal, antibacterial activities and in the treatment of tuberculosis infections [5,6]. It is well narrated that azomethine associated with active hydrazone moiety showed anticancer bioactivity [7]. Several metal complexes of hydrazone derivatives were screened for their biological and physiological activities against different bacterial and fungal species [8,9]. Naphthalimides were provoked to form a famous class of intercalating agents that consists of a flat, generally *p*-deficient aromatic or heteroaromatic system, which binds to DNA by insertion between base pairs of the double helix and generating a multitude of reactive intermediates that result in DNA cleavage [10].

The extensively studied mixed ligand cobalt(II)/copper(II) complexes with di-imines such as 1,10-phenanthroline as co-ligands tend to exhibit cytotoxic and antiviral activities upon interaction with nucleic acid templates and inhibit pro-viral DNA synthesis [11,12]. It is well known that *bis*(1,10-phenanthroline)-copper(II) binds to DNA non-covalently in the minor groove and shows an efficient DNA cleavage activity in the presence of thiol and hydrogen peroxide to generate active species that leads to DNA strand scission [13]. As there has been considerable interest in the design and study of DNA binding and cleavage properties of mixed-ligand Cu(II)/Co(II) complexes, [14,15] it is worthwhile to study these complexes as metallo-drugs.

On the other hand, an increasing interest in antioxidants, particularly in those intended to prevent the mischievous effects caused by free radicals in the human body is attracting one. The free radicals are also believed to be associated with carcinogenesis, mutagenesis, arthritis, diabetes, inflammation, cancer and genotoxicity [16,17] due to oxidative stress, which arises as a result of imbalance between free radical generations. The cytotoxic activity of a metal complex, which is closely related with its antitumor *viz.* antioxidant activity, is found to be induced by both the identity of the metal and the ligands bound to it [18]. Several research groups have reported the development of new metal-containing antioxidant agents [19,20]. All these properties were mainly associated with the presence of phenolic functions, which can show a general antioxidant and radical scavenging activity, more with the presence of the azomethine function. Such properties have gathered the interest in developing new hydrazone ligand and its copper/cobalt complexes as a biological agent, for their potential use in medicine *viz*. antioxidant and antimicrobial agents. The present paper reports, the synthesis of metal [Cu(II) and Co(II)] complexes with H_2bnp, phen and the characterization, nuclease activity, antioxidant and antimicrobial studies of the new metallo drugs.

2. Experimental

2.1. Materials and methods

ISSN 2153-2249 (Print) / ISSN 2153-2257 (Online)
DOI:10.5155/eurjchem.2.3.394-403.232

All reagents and chemicals were purchased from commercial sources (Sigma-Aldrich Co., Merck Co.) and used as received without further purification. Solvents used for spectroscopic measurements were purified by standard procedures [21]. Supercoiled (SC) pUC19 DNA and Calf thymus (CT) DNA were procured from Bangalore Genie (India). The buffer solution was prepared using deionized and sonicated triple-distilled water. The purity and identity of the prepared complexes were determined by means of elemental analysis, thermal analysis, ESI-MS, UV-VIS and FT-IR spectra.

2.1.1. Physical measurements

Melting points of the compounds in the capillary tubes were recorded and are uncorrected. Elemental analyses were carried out on an Elemental Vario EL elemental analyzer. The molar conductance data were recorded in 10^{-3} M dimethylformamide (DMF) solution at room temperature using an Elico CM-180 conductometer. The cell constant of the conductivity cell used was 0.5 cm^{-1}. The electrospray ion mass spectra (ESIMS) were recorded on API 2000 Applied Bio-system triple quadrupole mass spectrometer. The solution was introduced into the ESI source through a syringe pump at the rate 5 µL/min. The ^{1}H NMR spectra were recorded on a Brucker AV-400 MHz FT NMR spectrometer in DMSO-d_6. Infrared spectra were recorded in the range 4000-400 cm^{-1} on a Jasco FT/IR-4100 FT-IR spectrometer, by Nujol mull method. Electronic spectra were obtained with a Hitachi U-2000 Japan, recording spectrophotometer in DMF solutions at concentration of 10^{-3} M. Magnetic measurement were carried out by the Gouy method at room temperature (28 ± 2 °C) using $Hg[Co(SCN)_4]$ as the calibrant. TG and DTA were performed by using Universal V4.3A TA Instruments. Fluorescence spectra were recorded on a Shimadzu RF-5301pc spectrofluorimeter.

2.1.2. Preparation of ligand H_2bnp

The Schiff base H_2bnp was prepared as reported earlier [22], by refluxing the mixture of 15 mL each of the methanolic solution of 3-hydroxy-2-naphthoic hydrazide (0.005 mol) and salicylaldehyde (0.005 mol) for about 6 h with stirring. The completion of the reaction was monitored by TLC method, the yellow precipitate formed was filtered, washed with dry ethanol. The product was dried in vacuum. H_2bnp: Yield: 97%. M.p.: 316-318 °C. IR (Nujol mull, ν, cm^{-1}): 3442 (Ar-OH), 1644 (C=O), 1619 (C=N), 966 (N-N). ^{1}H NMR (300 MHz, DMSO-d_6, δ, ppm): 12.46 (s, OH), 8.53 (s, NH), 6.80-7.45 (s, ArH), 8.45 (s, HC=N). ESI-MS (m/z): 307 $[M+1]^+$. Anal. Calcd. for $C_{18}H_{14}N_2O_3$: C, 70.58; H, 4.61; N, 9.15. Found. C, 70.08; H, 4.65; N, 9.07%.

2.1.3. Preparation of $[Cu^{II}(phen)(bnp)H_2O]$ (1) and $[\{Co^{II}(phen)(bnp)H_2O\}H_2O]$ (2)

The mononuclear complexes **1** and **2** were prepared in good yield following a general procedure in which 10 mL each methanolic solution of heterocyclic base phen (0.005 mol) and copper(II)/cobalt(II) acetate (0.005 mol) was reacted, followed by the addition of a THF solution (15 mL) of H_2bnp (0.005 mol). The reaction mixture was refluxed for one day with stirring at 50 °C. The solution on slow evaporation gave the dark green and brown colored product for copper and cobalt complexes, respectively. The solid isolated with remaining solvent was filtered and washed with cold aqueous methanol and dried over P_4O_{10}.

Compound **1**: Yield: 86 %. M.p.: >300 °C. IR (Nujol mull, ν, cm^{-1}): 3443 (Ar-OH), 1606 (C=N), 1573 (C=N-N=C), 1168 (-N=C-O), 409 (M-O), 514 (M-N). ESI-MS (m/z): 567 $[M+1]^+$. Conductance (Λ, ohm^{-1} cm^2 mol^{-1}): 14.7. Anal. Calcd. for $C_{30}H_{23}CuN_4O_4$: C, 63.65; H, 3.92; N, 9.90. Found: C, 63.41; H, 3.84; N, 9.34%.

Compound **2**: Yield: 92 %. M.p.: >300 °C. IR (Nujol mull, ν, cm^{-1}): 3399 (Ar-OH), 1637 (C=N), 1585 (C=N-N=C), 1184 (-N=C-O), 417 (M-O), 537 (M-N). Conductance (Λ, ohm^{-1} cm^2 mol^{-1}): 24.3. ESI-MS (m/z): 680 $[M+1]^+$. Anal. Calcd. for $C_{30}H_{24}CoN_4O_5$: C, 62.18; H, 4.17; N, 9.67. Found: C, 62.04; H, 4.14; N, 9.46.

2.1.4. Preparation of $[Cu^{II}(Hbnp)_2]$ (3) and $[Co^{II}(Hbnp)_2]$ (4)

To a volume of 10 mL methanolic solution of copper(II)/cobalt(II) acetate (0.005 mol), a 15 mL of heterocyclic ligand H_2bnp (0.010 mol) solution in THF was added and the reaction mixture was refluxed for one day with stirring at 50 °C. The solution on slow evaporation gave the pale green and dark brown colored product for copper and cobalt complexes, respectively. The solid isolated with remaining solvent was filtered and washed with cold aqueous methanol and dried over P_4O_{10}.

Compound **3**: Yield: 78 %. M.p.: >300 °C. IR (Nujol mull, ν, cm^{-1}): 3440 (Ar-OH), 1621 (C=N), 1553 (C=N-N=C), 1195 (-N=C-O), 429 (M-O), 507 (M-N). ESI-MS (m/z): 674 $[M+1]^+$. Conductance (Λ, ohm^{-1} cm^2 mol^{-1}): 11.4. Anal. Calcd. for $C_{36}H_{26}CuN_4O_6$: C, 64.14; H, 3.89; N, 8.31. Found: C, 64.07; H, 3.84; N, 8.36%.

Compound **4**: Yield: 82 %. M.p.:>300 °C. IR (Nujol mull, ν, cm^{-1}): 3428 (Ar-OH), 1614 (C=N), 1571 (C=N-N=C), 1199 (-N=C-O), 412 (M-O), 544 (M-N). ESI-MS (m/z): 668 $[M+1]^+$. Conductance (Λ, ohm^{-1} cm^2 mol^{-1}): 9.7 Anal. Calcd. for $C_{36}H_{24}CoN_4O_6$: C, 64.77; H, 3.62; N, 8.39. Found: C, 64.1; H, 3.59; N, 8.32%.

2.2. DNA Binding and cleavage activities

2.2.1. Electronic absorption titration

Solutions of CT DNA in the buffer 0.050 mol NaCl/0.005 mol Tris HCl (pH = 7.2) prepared using deionized water gave a ratio 1.9:1 of UV absorbance at 260 and 280 nm (A_{260}/A_{280}), indicating that the DNA was sufficiently free from protein [23]. The concentration of CT-DNA was determined from its absorption intensity at 260 nm with a known molar absorption coefficient value of 6600 dm^3/mol.cm [24]. Stock solutions were stored at 4 °C and used over not more than 4 days. Absorption titration experiments were performed on a Hitachi U-2000 Japan by maintaining the metal complex concentration constant (20 µ mol) in 10 % DMF and varying the nucleic acid concentration (0-40 µ mol) with reference cell containing DNA alone to nullify the absorbance due to the DNA at the measured wavelength. This was achieved by dissolving an appropriate amount of the complex and DNA stock solutions while maintaining the total volume constant (2 mL). The absorbance of the most red-shifted band of each investigated complex was recorded after successive additions of CT DNA pretreated with the complex. From the absorption titration data, the binding constant was determined using the following equation [25],

$$[DNA]/(\varepsilon_a - \varepsilon_f) = [DNA]/(\varepsilon_b - \varepsilon_f) + 1/K_b(\varepsilon_b - \varepsilon_f) \quad (1)$$

where, ε_a, ε_f, and ε_b correspond to $A_{obs}/[Cu]$, the extinction coefficient for the free complex, and the extinction coefficient for the complex in the fully bound form, respectively. A plot of $[DNA]/(\varepsilon_a - \varepsilon_f)$ versus [DNA], gives K_b (binding constant) as the ratio of the slope to the intercept.

2.2.2. Fluorescence spectroscopy

Emission intensity measurements were carried out on a Shimadzu RF-5301pc spectrofluorimeter for the relative binding of complex with an EB (ethidium bromide) bound CT-DNA solution in 0.005 mol Tris-HCl/0.050 M NaCl buffer (pH = 7.2). Tris buffer was used as the blank to make preliminary adjustments. DNA was pretreated with ethidium bromide in the ratio of 0.1 ([EB] = 0.5 x 10^{-5} mol, [CT-DNA] = 5 x 10^{-5} mol) for 30 min at 27 °C. The different complex concentrations in 10 % DMF ranging from 2 to 5 x 10^{-5} mol were then added to this mixture and their effect on the emission intensity was measured at 603 nm (excitation at 512 nm). The quenching constant K_{sv} was deduced from Stern-Volmer method where the ratio of fluorescence of the compound alone (F_0) over the fluorescence of the compound in the presence of CT-DNA (F) is presented as a function of CT-DNA concentration.
In this configuration,

$$F_0/F = 1 + K_{sv}[Q] \quad (2)$$

The slope K_{sv} is considered as an equilibrium constant for the static quenching process and [Q] is the concentration of the quencher.

2.2.3. Viscosity measurement

For viscosity measurements an Ubbelodhe viscometer was thermostated at 28.0 ± 0.1 °C in a constant temperature bath. The concentration of DNA was 50 μM and the flow time was measured with a digital stopwatch, at different loadings of the complexes. Each sample was tested three times to get an average calculated flow time. Data were presented as $(\eta/\eta_0)^{1/3}$ versus binding ratio ($1/R$ = [Cu]/[DNA] = 0.0-0.5), where η is the viscosity of DNA in the presence of complex, η_0 being the viscosity of free DNA solution alone. The viscosity values were calculated from the observed flow time of CT-DNA containing solutions (t) duly corrected for that of the buffer alone (t_0), $\eta_0 = (t - t_0)/t_0$.

2.2.4. Cleavage efficiency

The DNA cleavage activity of the metal complexes was studied by using agarose gel electrophoresis. Supercoiled plasmid pUC19 DNA (50 µmol) was dissolved in a 0.050 mol tris-(hydroxymethyl) methane-HCl (Tris-HCl) buffer (pH = 7.2) containing 0.050 mol NaCl and the different concentration of complexes (100, 200, 300 and 400 µmol). The mixtures were incubated at 37 °C for 24 h and then mixed with the loading buffer (2 µL) containing 25 % bromophenol blue, 0.25 % xylene cyanol and 30 % glycerol. Each sample (5 µL) was loaded into 0.8 % w/v agarose gel. Electrophoresis was undertaken for 1 h at 50 V in tris-acetate-EDTA (TAE) buffer. The gel was stained with ethidium bromide for 5 min after electrophoresis, and then photographed under UV light. The proportion of DNA in each fraction was quantitatively estimated from the intensity of each band with the Alpha Innotech Gel documentation system (AlphaImager 2200). To enhance the DNA cleaving ability by the complexes, hydrogen peroxide (100 µ mol) was added into each complex (400 µmol). Moreover, the cleavage mechanism was further investigated by using scavengers for the hydroxyl radical species (4 µL, DMSO) and the singlet oxygen species (100 µ mol, NaN_3). All experiments were carried out in triplicate under the same conditions.

2.2.5. Free radical scavenging activity by DPPH assay

The free radical-scavenging activity of the compound was measured in terms of hydrogen donating or radical-scavenging ability using the stable radical DPPH described by Blois method [26]. Briefly, stock solutions of the samples (0.001 g/mL) were prepared by dissolving in DMSO. Different concentrations (20-100 µL) of stock solution were make up to 3 mL with methanol. Solution of DPPH (0.0001 mol) in methanol was prepared and 1 mL of this solution was added to the above each test solutions. The mixture was shaken vigorously and incubated for 30 min and then at 517 nm the absorbance was measured. All the tests were run in triplicate and expressed as the mean±standard deviation (S.D.). Ascorbic acid (AA) was used as a standard or positive control, parallel to the test compound and in the absence of test compound/standard used as the negative control. The capability to scavenge the DPPH radical was calculated using the following equation:

$$DPPH^{\cdot} \text{ scavenging effect } (\%) = [(A_c - A_b/A_c) \times 100] \quad (3)$$

where A_c is absorbance of the negative control *i.e.* without sample; A_b is the absorbance with the sample.

2.2.6. Hydroxyl radical scavenging assay

The ability of the compounds to effectively scavenge hydrogen peroxide, determined according to the method of Ruch *et al.* [27], where it is compared with that of butylated hydroxyanisole (BHA) as standard. The hydroxyl radicals (OH^-) in aqueous media were generated through the Fenton system. The solution of the tested compound was prepared with DMSO (0.001g mL^{-1}). The 5 mL assay mixture contained following reagents: safranin (11.4 µmol), EDTA-Fe(II) (40 µ mol), H_2O_2 (1.76 µ mol), the tested compound (4-20 µL) and a phosphate buffer (0.067 mol, pH = 7.4). The assay mixtures were incubated at 37 °C for 30 min in a water bath. After which, the absorbance was measured at 520 nm. BHA was used as standard compound for suppression of hydroxyl radical. All the tests were run in triplicate and expressed as the mean±standard deviation (S.D.). The suppression ratio for $OH^{\cdot}$ was calculated from the following expression:

$$\text{Supression ratio } (\%) = \frac{A_o - A_i}{A_o} \times 100 \quad (4)$$

where, A_0 = the absorbance of the control; A_i = the absorbance in the presence of the tested compound.

2.2.7. Antibacterial assays

The complexes and ligands were tested for their in vitro antibacterial activity against *Escherichia coli, Staphylococcus aureus, Xanthomonas vesicatoria* and *Ralstonia solanacearum* strains. Initial screening of compounds was performed by following disc diffusion method. Suspensions in sterile distilled water from 24 h cultures of microorganisms were adjusted to 0.5 McFarland. Muller-Hinton Petri dishes of 90 mm were inoculated using these suspensions. Paper disks (5 mm in diameter) containing 100 µL of the substance to be tested (at a concentration of 0.002 g/mL in DMF) were placed at the edge of the Petri plates containing Nutrient agar (NA). One 5 mm diameter agar disc of test organism from a one week old NA culture was placed in the centre of the plate. Incubation of the plates was done at 37 °C for 24 h. Reading of the results was done by measuring the diameters of the inhibition zones generated by the tested substances, using a ruler. Chloramphenicol was used as a reference substance.

The *in vitro* anti-fungal assay was performed by the disc diffusion method. The complexes and ligand were tested against the fungi *Aspergillus niger* and *Aspergillus flavus*, cultured on potato dextrose agar as medium. In a typical procedure, a well was made at the center on the agar medium inoculated with the fungi. The well was filled with the test solutions (100 µL) using a micropipette and the plate was incubated at 37 °C for 72 h.

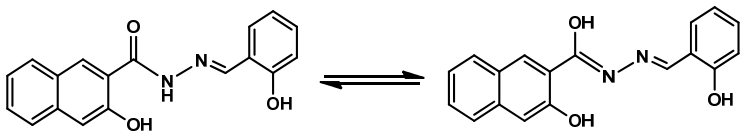

Keto (I) and Enol (II) tautomeric form of H_2bnp

Scheme 1

During this period, the test solution diffused and the growth of the inoculated fungi was affected. The inhibition zone developed on the plate was measured. Fluconazole was used as a reference compound.

The prepared compounds were further used to determine minimum inhibitory concentration (MIC) in 96 well, sterile, flat bottom microtiter plates, based on broth micro dilution assay, which is an automated colorimetric method, uses the absorbance (optical density) of cultures in a microtiter plates [28]. Each well of microtiter plates was filled with 200 µL of nutrient broth/potato dextrose broth, 1µL of test organism and 15µL of different concentration of selected compounds. For bacteria and fungi the microtiter plates were incubated at 35 ± 2 °C for 24 h. After the incubation period, the plates were read at 610 nm using ELISA reader (ELX 800 MS, Biotek instruments, Inc. USA). MIC, which was determined as the lowest concentration of compound inhibiting the growth of the organism, was determined based on the optical density.

3. Result and discussion

3.1. Chemistry

Treatment of Cu(II)/Co(II) acetate with mixture of ligands i.e. 1,10-phenonthraline and H_2bnp in 1:1:1 ratio, and with same ligands H_2bnp in 1:2 ratio at reflux condition for one day led to the formation of a homogenous solution, work up of which gave the mononuclear complexes. Satisfactory analytical results were obtained for all the complexes, exhibiting paramagnetic character comparable to mononuclear copper(II)/cobalt(II) complexes of tridentate Schiff bases [29]. The FAB mass spectrum of H_2bnp and its complexes (**1**-**4**) showed important cluster peak assignable to the respective parent ion. The ligand H_2bnp is soluble in THF, CH_3CN, DMSO and DMF, whereas the complexes were soluble in DMSO and DMF. The complexes were stable in aqueous/tris-HCl buffer DMSO medium. Conductivity measurement was performed in DMF ($1x10^{-3}$ M) to establish the charge of the complexes. The molar conductivity (Λ) values of all the complexes fall in the range 9.7-24.3 ohm^{-1} cm^2 mol^{-1}, which is in agreement with non-electrolytic nature of the complexes [30].

3.1.1. ^{1}H NMR data

Usually hydrazone compounds like H_2bnp used in the present study may exist in the keto (I) or in the enol (II) tautomeric form in the solid state (Scheme 1). The obtained values for ^{1}H NMR chemical shifts of the ligand are comparable with previously reported for similar compounds [31]. In the ^{1}H NMR spectra of the H_2bnp having the naphtholic OH, phenolic OH and amide NH resonances appear as a singlet at δ 12.46, 14.24 and 8.54 ppm, respectively. The movements of naphtholic OH proton absorptions to lower frequency can be explained by strong intramolecular hydrogen bonding in this ligand. These findings indicate that the ligand is present in the ketonic form in the solid state. The azomethine resonance occurred at δ 8.45 ppm for H_2bnp.

3.1.2. IR spectra

The infrared spectra of the ligand H_2bnp and its complexes were measured using the Nujol technique in the range of 400-4000 cm^{-1}. The IR spectra of the azomethine ν(C=N_{imine}) group in ligand at 1619 cm^{-1} is shifted to 1621-1599 cm^{-1} upon its complexation process with metal salts, indicating coordination of metal with imine. Generally, hydrozen type ligands exist in two types of isomers, which have intramoleculer hydrogen bonding (Scheme 2). Parallel to the ^{1}H NMR spectral data, IR spectra of the NH stretching band of the ligand H_2bnp at 2393 cm^{-1} was merged probably due to overlapping with intramolecular hydrogen bonded NH···O (Isomer **I**), stretching frequencies. This condition exists commonly for aromatic azomethine compounds containing *o*-OH group [32]. For the IR spectral band of H_2bnp, the ν(C=O) stretching vibration appeared at lower frequency (1644 cm^{-1}) than usual value [33]. This phenomenon may be explained for the strong intramolecular hydrogen bonding (OH···O) between the carbonyl group of H_2bnp and the phenolic OH group in isomer **II** (Scheme 2). Upon complexation, the two new bands appear between 1573-1514 and ~1168-1199 cm^{-1}, probably due to ν(C=N-N=C) and ν(N=C-O), respectively, suggesting that the NH proton is lost via enolization and the resulting enolic oxygen and the azomethine nitrogen take place in coordination.

The IR spectra of complexes derived from H_2bnp show a characteristic small broad band for phenolic OH group around 3450 cm^{-1} due to the effect of intramolecular hydrogen bonding. Upon complexation, a broad band in the region 3399 cm^{-1} occurred for complexes **1** and **2**, which can be attributed to the presence of coordinated water molecule, whereas for **3** and **4** this band is not appeared indicating absence of water molecule. This fact is supported by the observation of the thermal analysis data. The new bands existed at 402-429 and 500-555 cm^{-1} provide additional proof for M-O and M-N bond formation.

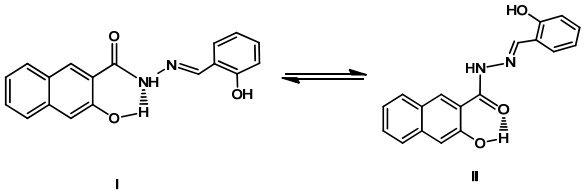

I II

Scheme 2

3.1.3. UV-visible spectral and magnetic moment studies

The UV-Vis spectral data of the ligand H_2bnp and its metal complexes were collected by dissolving in DMF (10^{-3} mol/dm^3) solution. The absorption spectrum of Schiff base is characterized mainly by three absorption bands in the region 284-330 nm which may be assigned to π-π* and n-π* transition associated within the C=N and C=O bonds influenced by charge transfer interaction and the longer wavelength band at 397 nm

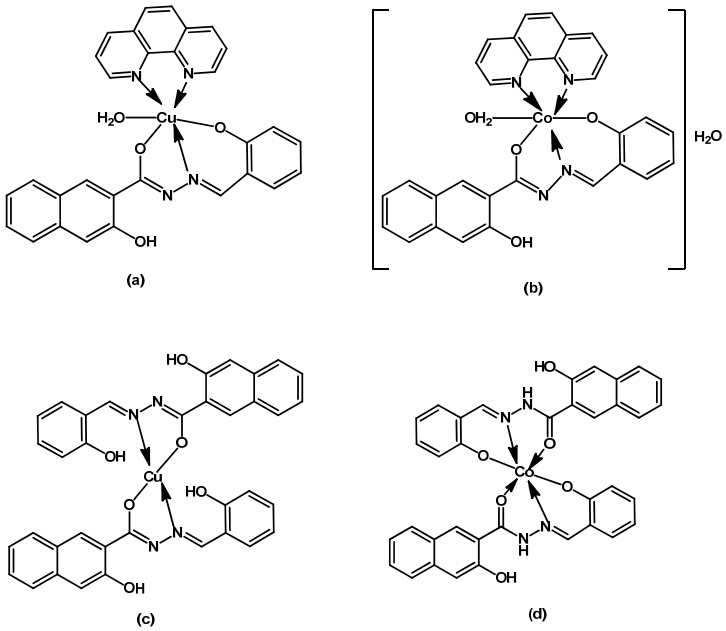

Possible structures of (a) Complex 1 (b) Complex 2 (c) Complex 3 and (d) Complex 4

Scheme 3

is assigned to intramolecular charge transfer transition of phenolic OH [34].

The UV-Vis spectra of complexes do not resulted in strong modification. However, small modifications in the intensity and in the wavelength occur as a result of electron transition upon complexation. The strong band observed in the range 275-295 nm is due to an intra-ligand charge transfer transition for all the complexes.

The weak broad absorption band in the range 308-335 nm may be assigned to the electronic transition associated with the CH=N- linkages, as a contribution from both mixed and similar ligands. The electronic spectra of **3** exhibit characteristic absorption curves corresponding to a square-planar geometry. Generally for square-planar complexes with a $d_{x^2-y^2}$ ground state, three spin-allowed transitions are expected, *viz*. $^2B_{1g} \rightarrow {}^2A_{2g}$ ($d_{x^2-y^2} \rightarrow d_{z^2}$), $^2B_{1g} \rightarrow {}^2B_{2g}$ ($d_{x^2-y^2} \rightarrow d_{xy}$) and $^2B_{1g} \rightarrow {}^2E_g$ ($d_{x^2-y^2} \rightarrow d_{xz,yz}$) which are very close in energy [35]. However, an intense broad band is occurred for complex **1** and **3** around 390 nm for LMCT band, a characteristic feature usually associated with metal-hydrazone complexes [36]. The absorption maxima at 400-440 nm for complexes **2** and **4** is assigned to the transition $^4T_{1g}(F) \rightarrow {}^4T_{1g}(P)$ (ν_3) suggesting octahedral structure around Co(II) ion [37]. Notably, the expected *d-d* absorption band of the cobalt(II) ion for complexes **2** and **4** is not observed may be lost in the low energy tail of the charge transfer transition.

The magnetic moment value (1.98 BM) of the complex **1** supports the presence of distorted octahedral structure, in which water molecule occupies the apical position, while that of complex **3** show the magnetic value of 1.82 BM corresponding to single unpaired electron reflecting square planar geometry [38]. The magnetic moment values of Co(II) complexes **2** and **4** have been found to be 4.68 and 5.03 BM, respectively showing three unpaired electrons which is within the range of values corresponding to high spin (sp^3d^2 structure) octahedral complexes of Co(II) ion [39,40]. The slight deviation observed with respect to the spin-only value is attributable to the orbital contribution. Based on the above spectral data expected structures for the prepared complexes were presented in Scheme 3.

3.1.4. FAB mass and thermal study

The ligand H_2bnp and its complexes were analyzed by ESI-MS, in methanolic solution and positive mode. For H_2bnp the main peak is observed at m/z$^+$ 307 and assigned to [H_2bnp +H]. Whereas the main peaks at m/z$^+$ 567, 580, 674 and 668 were appeared for the complexes (**1**) [Cu(bnp)(phen)H_2O +H], (**2**) [Co(bnp)(phen)2H_2O +H], (**3**) [Cu(Hbnp)$_2$ +H] and (**4**) [Co(Hbnp)$_2$ +H], respectively. This technique became useful to show the obtained structure of mononuclear complexes in a 2:1 ratio (ligand: metal), and supporting data for the elemental analyses.

The TG measurements of the complexes **2** and **4** were performed in air over the temperature range of 20-1000 °C (Figure 1). The complex **2** was stable up to 98 °C. The existence of an anhydrous complex from [Co(bnp)(phen)(H_2O)].H_2O can be evident from the sample weight decreases up to 171 °C which is probably connected with the elimination of the water molecule present in complex **2**, leading to the formation of [Co(bnp)(phen)] species (weight loss: found 6.4 %, calcd. 5.29 %). The next decay starts at 172 °C and proceeds in two steps, forming two plateaus at 259 and 318 °C without formation of thermally stable intermediates up to 390 °C (weight loss: found 86.4 %, calcd. 83.62 %). A consecutive weight decrease can be seen between 395 and 500 °C which may be related to the formation of CoO (weight loss: found 13.1 %, calcd. 13.6 %).

The thermogravimetric curves of the complex **4** start to decompose at 385 °C in two successive steps. This sequence specifies the absence of water molecules in the complex moiety. The weight loss in the range 380-490 °C (weight loss: found 88.2 %, calcd. 90.6 %) indicated the decomposition of two numbers of Hbnp ligand with two plateaus and leaving behind its cobalt oxide residue.

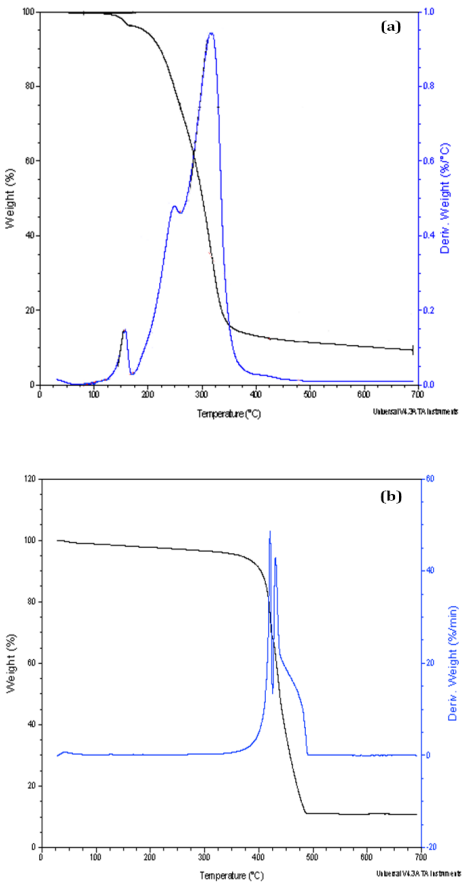

Figure 1. TG-DTG curves of Complex 2 (a) and Complex 4 (b).

3.2. Biological investigation

3.2.1. DNA binding studies

The binding of intercalative drugs to DNA helix has been characterized classically through absorption spectral titrations, by following the changes in absorbance and shift in wavelength.

The absorption spectra of the complex **1**, in the absence and presence of CT-DNA ([complex] = 20 μM, [DNA] = 0-40 μM) is presented in Figure 2. Upon increment of DNA concentration the intense absorption band appeared in the UV spectra at 265 nm for complex **1** exhibits hypochromism of about 17.6 % with slightly red shifts of 4 nm, which reveal the intra ligand π-π* transition of phen compound. This fact is attributed to the strong stacking interaction between aromatic phen chromophore group of the complex **1** and the base pairs of DNA. The binding constant K_b (4.35 x 10^5 M^{-1}) for complex **1,** was determined from the plot of [DNA]/(ε_a - ε_f) vs. [DNA] (Figure 2b) using the absorption value at 265 nm. Another UV absorption band appeared at 297 nm for charge transfer band and not showed any superior hypochromicity. While for the complex **2** an intense absorption bands appeared at 268, 321 and 417 nm upon increasing the concentration of DNA with no red shift, suggesting poor intercalation with the DNA base pairs. The binding constant K_b for complex **2** was found to be 6.6 x 10^4 M^{-1} at 268 nm, with the hypochromicity of about 10.34 %. The extent of hypochromism and red-shift observed for the mixed ligand complexes **1** and **2** are better comparing with the literature work [41,42] and lower than those observed for typical classical intercalators such as ethidium bromide (K_b, 1.4 x 10^6 M^{-1} in 25 mM Tris-HCl/40 mM NaCl buffer, pH = 7.9) [43] bound to CT DNA.

Conversely, absorption intensity of the complexes **3** and **4** increased (hyperchromism) evidently after the addition of DNA without any red shift of absorption band in the regions of 316-338 and 404-427 nm, assigned to π-π* transitions of the larger conjugated organic molecules and π-π* of the C=N-N=C groups coupled with charge transfers from ligands to metal ions (L→M), respectively, which indicated the interactions between DNA and the complex.

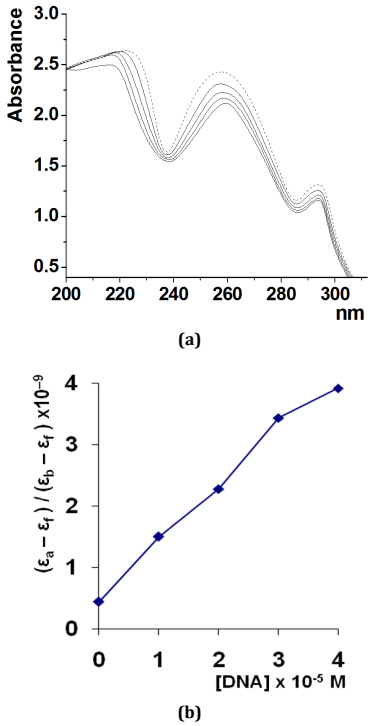

Figure 2. (a) Absorption spectra of complex **1** in tris-HCl buffer upon addition of increasing concentration of CT-DNA [0-40 μM]. [Complex] = 20 μM; (b) the non-linear least squares fit of $\Delta\varepsilon_{af}$ /$\Delta\varepsilon_{bf}$ *vs.* [DNA]/μM using McGhee-von-Hippel equation.

A similar hyperchromism was also observed for a copper(II) complex with a ligand bearing -OH group [44]. As DNA double helix possesses many hydrogen bonding sites which are accessible both in the minor and in the major grooves, it is likely that the -OH group of the ternary complex forms hydrogen bonds with DNA, which may contribute to the hyperchromism observed in absorption spectra. The very small change in the absorption intensity of MLCT band of complexes **3** and **4** on introducing CT DNA is consistent with its weak external contact with the duplex. The binding constant K_b for complexes **3** and **4** are found to be 6.35 x 10^3 M^{-1} and 2.2 x 10^3 M^{-1}, respectively.

The difference in the value of hypochromism or hyperchromism with a hypsochromic shift and the binding constant, from mixed ligand complexes to similar ligand complexes suggests that the type of binding mode is different. This may be attributed to a change in structure as well as the active functional group present in it. The binding nature in the mixed ligand complexes is significant due to π-stacking or a hydrophobic interaction of the aromatic diimine phen bases. Particularly the binding constants of complex **1** is sufficiently high, possibly due to its distorted square-based coordination geometry around copper(II) [45].

3.2.2. Viscosity measurements

Due to its sensitivity to the change in length of DNA, viscosity measurement is regarded as the least ambiguous and most effective test to study the binding mode of complex to DNA, especially in the absence of crystallographic structure data. A significant increase in the viscosity of DNA on the addition of complex indicates the intercalative mode of binding to DNA. In contrast, complex that binds in the DNA grooves by partial and/or non-classical intercalation cause less pronounced (positive or negative) or no change in DNA solution viscosity.

The changes of relative viscosity of rod-like CT-DNA in the presence of complexes **1**-**4** are shown in Figure 3. The ability of the complexes to increase the viscosity of DNA depends upon the diimine ligand (phen). The partial intercalation of the phen ring of complex **1** and **2** in between the DNA base pairs also leads to untwisting and increase in separation of base pairs at intercalation sites leading to an increase in overall DNA contour. These results parallel the hypochromism and K_b values observed for the complexes **1** and **2**. However, complexes **3** and **4** appear to block the intercalative interaction strongly and hence the negligible changes in the relative DNA viscosity observed. This is in conformity with its lowest DNA binding affinity. Similarly, the presence of hydroxyl group on the naphthyl ring would also sterically hinder the partial insertion of the Hbnp ring in between the DNA base pairs, leading to no change in relative viscosity of DNA and possibly the formation of kinks or bends on the DNA contour length.

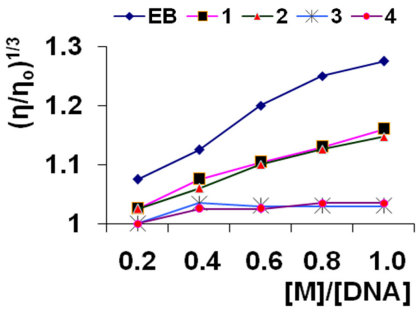

Figure 3. Effect of increasing the concentration of the complexes **1** (■), 2 (▲), 3 (•), 4 (●) and EB (♦) on the relative viscosities of CT-DNA at 28.0 ± 0.1 °C in 5 mM tris-HCl buffer (pH = 7.2).

3.2.3. Fluorescence study

No luminescence was observed for complexes at room temperature in aqueous solution, in any organic solvent examined, or in the presence of CT-DNA. So the binding of complexes cannot be directly presented in the emission spectra. To further clarify the interaction of the complex with DNA, the competitive binding experiment was carried out. EB is one of the most sensitive fluorescent probes that can bind with DNA. There is an increase in the fluorescence of EB due to intercalation with DNA. If the metal complex intercalates with DNA it leads to a decrease in the binding sites of DNA available for EB, which is reflected, from a decrease in the fluorescence of the EB-DNA system. The fluorescence quenching of EB bound to CT-DNA by complexes **2** and **3** is shown in Figure 4. The addition of complex to EB-bound CT-DNA solution caused obvious reduction in emission intensities, indicating that complexes competitively bound to CT-DNA with EB. The extent of reduction of the emission intensity gives a measure of the binding propensity of the complex to CT-DNA.

The observed enhancement in induced emission intensity of EB bound to DNA decreases in the order, complexes **1** (67 %) > **2** (52 %) > **3** (32 %) > **4** (28 %) which is consistent with the results from spectral and viscosity measurements. This reflects the ability of the complexes to displace the DNA-bound EB and thus complex **1** and **2** are effectively hinders the enhancement in EB emission suggesting its strong competition with EB for the intercalative binding site. The presence of biphenyl-OH groups sterically hinders the partial intercalation of the biphenyl moiety and permits the solvent water molecules to enter the DNA molecule and deactivate the intercalating activity of complexes **3** and **4**. The lower K_b value and small change in fluorescence spectral studies indicate the non-intercalative binding interaction with DNA and probable groove binding or external binding is suggested for complexes **3** and **4** [46], which is supported by viscosity measurements not to be involved in intercalative binding but report in groove binding.

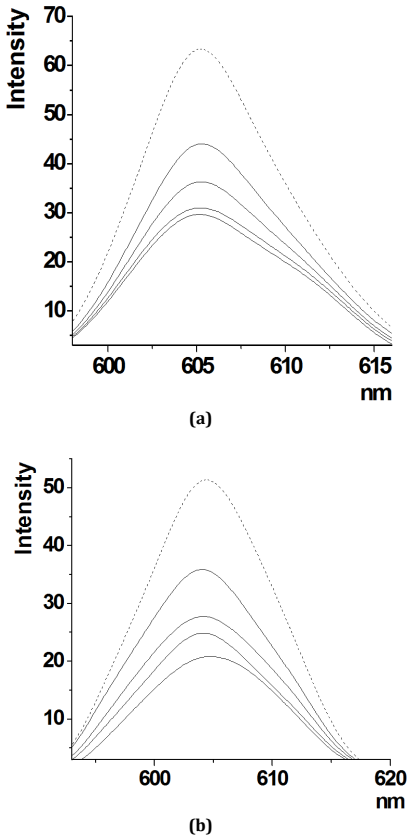

Figure 4. Emission spectrum of EB bound to DNA in the absence (doted line) and presence of increasing complex (a) **2** and (b) **3** concentration ([EB] = 0.5 x 10^{-5} mol, [CT-DNA] = 5 x 10^{-5} mol [complex] = 0-5 x 10^{-5} mol, λ_{ex} = 512 nm).

According to the classical Stern-Volmer equation [47], the Stern-Volmer constant K_{SV} used to evaluate the quenching efficiency is obtained as the slope of F_0/F versus complex concentration linear plot. From the Figure 5, the K_{SV} value for the complexes **1** and **2** is 5.45 x 10^4 M^{-1} and 1.13 x 10^4 M^{-1}, respectively. The quenching plot illustrates that the quenching of EB bound to DNA by complexes is in agreement with the linear Stern-Volmer equation, which also indicates the complexes **1** and **2** binds to CT-DNA in an intercalative mode. It may be due to the complex interacting with DNA through intercalation binding, so releasing some free EB from the EB-DNA complex, which is consistent with the above absorption spectral result. The complexes **3** and **4** did not satisfied linear Stern-Volmer equation, having the K_{SV} value of 1.45 x 10^3 M^{-1} and 1.33 x 10^3 M^{-1}, respectively indicating non-intercalation binding mode.

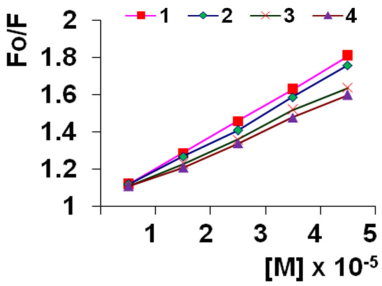

Figure 5. Plot of F_0/F *vs.* [complex] for the titration of the complexes **1** (■), **2** (♦), **3** (x) and **4** (▲) to CTDNA-EB system.

3.2.4. DNA-cleavage activity

The degree to which the four complexes could function as DNA cleavage agents was examined using supercoiled pUC19 plasmid DNA as the target. The efficiency of cleavage of these molecules was probed using agarose gel electrophoresis. When circular plasmid DNA is conducted by electrophoresis, the fastest migration will be observed for the supercoiled form (Form **I**). If one strand is cleaved, the supercoil will relax to produce a slower-moving nicked circular form (Form **II**). If both strands are cleaved, a linear form (Form **III**) will be generated that migrates in between. Complexes **1**-**4** were found to promote the cleavage of pUC19 plasmid DNA from supercoiled Form (**I**) to the nicked Form (**II**) by varying the concentration (100-400 µM, figure not presented). The complexes can induce the obvious cleavage of the plasmid DNA at the concentration of 100 µM. Under comparable experimental conditions, complexes exhibit effective DNA cleavage activity in the following order **1** > **3** > **2** > **4**. The different DNA-cleavage efficiency of the complexes may be due to the different binding affinity of the complexes to DNA.

One of the most interesting electrophoretic results of the complexes takes place when experiment done in presence of H_2O_2, where the cleavage of the supercoiled DNA Form (**I**) into nicked DNA Form (**II**) take place more than complex alone. The mechanism of pUC19 DNA cleavage by complexes **1**-**4** was then studied by implementing various inhibiting reagents. The effect of reactive oxygen species on this process was tested with standard hydroxyl radical scavenger (DMSO) and singlet oxygen scavenger (NaN_3). DMSO (lanes 5 and 8 in Figure 6a and 6b) remarkably inhibited the DNA breakage (34-41 %) induced by the complexes (100 µM). Based on these data, hydroxyl radicals clearly mediate DNA damage produced by complexes **1**-**4**. Interestingly, the singlet oxygen scavenger NaN_3 failed to protect the DNA from complexes **1**-**4** induced cleavage almost (lanes 6 and 10, Figure 6a and 6b), which suggests that singlet oxygen does not play an important role in the cleavage mechanism pathway. In summary, these results indicate that the cleavage reaction involves hydroxyl radicals that is, a Fenton type reaction may leads to the formation of these oxygen active species which finally cleave the DNA.

3.2.5. Free radical-scavenging capacity (RSC)

The RSC of the newly synthesized compounds was evaluated by measuring the scavenging activity against 2,2-diphenyl-1-picrylhydrazyl (DPPH) radical and by neutralization of hydrogen peroxide. The DPPH radical is one of the most commonly used substrates for fast evaluation of antioxidant activity because of its stability and simplicity of the assay. On the contrary a non-free radical species, hydrogen peroxide is the source of the very toxic hydroxyl radical, especially in the presence of metal ions such as copper or iron. Also, hydrogen peroxide can cross membranes and may slowly oxidize a number of cell compounds leading to cause death. Thus, the elimination of hydrogen peroxide, as well as hydroxyl radical, is important for both, human health and the protection of food systems.

3.2.6. DPPH-scavenging activity

In the DPPH assay, the ability of the investigated H_2bnp and its Cu(II)/Co(II) complexes, to act as donors of hydrogen atoms or electrons in transformation of DPPH radical into its reduced form DPPH-H was investigated. The dissociation energy of the OH bond is considered to be one of the most important physico-chemical parameters involved in the definition of the antioxidant potency of phenolic derivatives. Phenols are also excellent chain-breaking antioxidants and good $^1O_2$ quenchers [48]. The ability of the compounds to effectively scavenge DPPH radical is displayed in Figure 7, where it is compared with that of ascorbic acid as standard. H_2bnp was able to reduce the stable, purple-coloured radical, DPPH into the yellow coloured DPPH-H reaching 50% of reduction, and then the absorbance was measured at 517 nm. Lower absorbance values of the reaction mixture indicated higher free radical scavenging activity. The IC_{50} value of the H_2bnp was found to be more than the standard, Ascorbic acid. While this activity was reduced for the complexes in the order **2** > **1** > **4** > **3** and the IC_{50} values were presented in Table 1.

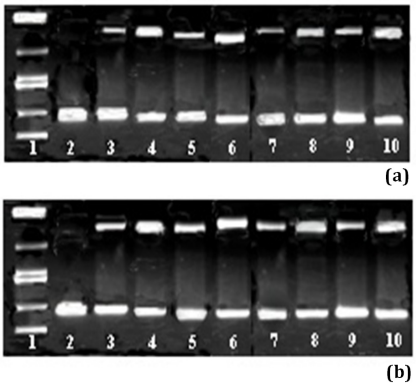

Figure 6. Cleavage of SC pUC19 DNA (50 μM) by complexes **1**-**4** (100 μM) in the presence of H_2O_2 (100 μM), in 10 mM tris-HCl/1 mM EDTA buffer (pH=8.0). **(a)** lane 1, DNA Marker; lane 2, DNA control; lane 3 and 7, DNA + complex **1** and DNA + complex **2**, respectively; lane 4 and 8, DNA + complex **1** + H_2O_2 and DNA + complex **2** + H_2O_2, respectively; lane 5 and 9, DNA + complex **1** + H_2O_2 + DMSO (4 µL) and DNA + complex **2** + H_2O_2 + DMSO (4 µL), respectively; lane 6 and 10, DNA + complex **1** + H_2O_2 + NaN_3 (100 μM) and DNA + complex **2** + H_2O_2 + NaN_3 (100 μM), respectively. **(b)** lane 1, DNA Marker; lane 2, DNA control; lane 3 and 7, DNA + complex **3** and DNA + complex **4**, respectively; lane 4 and 8, DNA + complex **3** + H_2O_2 and DNA + complex **4** + H_2O_2 respectively; lane 5 and 9, DNA + complex **3** + H_2O_2 + DMSO (4 µL) and DNA + complex **4** + H_2O_2 + DMSO (4 µL), respectively; lane 6 and 10, DNA + complex **3** + H_2O_2 + NaN_3(100 μM) and DNA + complex **4** + H_2O_2 + NaN_3 (100 μM), respectively.

Table 1. Minimum percentage inhibitory concentration of DPPH radical and hydrogen peroxide by H_2bnp and its complexes (**1**-**4**).

Compound	IC_{50} (µ mol)±S.D.*	
	DPPH	H_2O_2
H_2bnp	92±0.34	14±0.21
1	105±0.56	23±0.15
2	102±0.31	20±0.42
3	112±0.05	28±0.25
4	108±0.52	27±0.40
AA	99±0.33	-
BHA	-	17±0.14

*S.D.: Standard deviation (average of three replicates).

Table 2. *In vitro* antimicrobial results of H_2bnp and its metal complexes.

Compounds	Inhibition zone in mm for bacteria*				Inhibition zone in mm for fungi*	
	S. aureus	*X. vesicatoria*	*R. solanacearum*	*E. coli*	*A. niger*	*A. flavus*
H_2bnp	08	14	10	21	27	23
1	46	53	48	51	47	54
2	37	47	45	48	51	49
3	22	32	25	32	35	38
4	23	28	27	29	30	34
Chloramphenicol	180	200	230	250	--	--
Fluconazole	--	--	--	--	280	290

* The results obtained were the average of three replicates with the concentration of 200 µg/mL.

Table 3. Minimum inhibitory concentration (IC_{50}) results of H_2bnp and its complexes for antimicrobial activity* in µg/mL.

Compound	*S. aureus*	*X. vesicatoria*	*R. solanacearum*	*E. coli*	*A. niger*	*A. flavus*
H_2bnp	>100	>100	>100	>100	>100	>100
1	64	47	82	42	38	44
2	88	54	83	57	46	43
3	100	97	92	>100	72	69
4	>100	85	66	>100	90	75
Chloramphenicol	20	20	20	20	-	-
Fluconazole	-	-	-	-	20	20

* The results obtained were the average of three replicates.

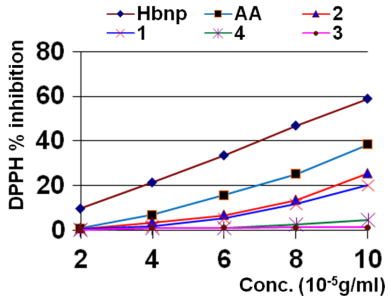

Figure 7. DPPH radical scavenging capacity of H_2bnp and its complexes (**1**-**4**) at different concentrations. Each value is the average of triplicates, representing ±S.D..

It has been reported that oxidative stress, which occurs when free radical formation exceeds the body's ability to protect itself, forms the biological basis of chronic conditions such as arteriosclerosis [49]. Based on the data obtained from the DPPH assay study, free radical scavenging activity increases with increasing concentration and ligand H_2bnp found to be an excellent antioxidant than its complexes **1**-**4**, suggesting the involvement of both phenolic and naphtholic hydroxyl groups in the DPPH radical scavenging process.

3.2.7. Hydrogen peroxide-scavenging assay

Scavenging of H_2O_2 by H_2bnp may be attributed to its phenolic group, which can donate electrons to H_2O_2 thus neutralizing it to water. The differences in H_2O_2 scavenging capacities between the H_2bnp and its complexes **1**-**4** may be attributed to the structural features of their active components, which determine their electron donating abilities. The ability of the compounds to effectively scavenge hydrogen peroxide is displayed in Figure 8, where it is compared with that of BHA as standard. The H_2bnp is capable of scavenging hydrogen peroxide in a concentration dependent manner. H_2bnp exhibited IC_{50} value at the concentration of 14±0.21 µmol for hydrogen peroxide scavenging activity, whereas, the BHA showed IC_{50} value at 17±0.14 µmol. While this activity was reduced for the complexes in the order **2** > **1** > **4** > **3** and the IC_{50} values were presented in Table 1. This type of antioxidant activity for cobalt complexes was correlated in literature work [19].

Although hydrogen peroxide itself is not very reactive, it can sometimes cause cytotoxicity by giving rise to hydroxyl radicals in the cell. Hydroxyl radicals are the major active species that cause lipid oxidation and significant biological damage thus, removing H_2O_2 is very important throughout food systems [50]. In this context, this type of antioxidant method becomes very useful in the development of pharmacological field.

The correlation between the H_2bnp and its complexes values and those of the control was statistically significant (p < 0.05).

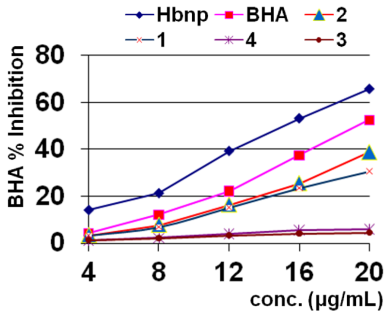

Figure 8. H_2O_2 scavenging activity of H_2bnp and its complexes (**1**-**4**) at different concentrations; each value is the average of triplicates, representing ±S.D..

3.2.8. Antibacterial assays

The antimicrobial activities of H_2bnp and its complexes **1**-**4** were tested by the agar well diffusion method and the results are presented in Table 2 and its MIC values in Table 3. The activity of these compounds against four different types of bacteria and fungi, namely *E. coli, S. aureus, X. vesicatoria, R. solanacearum* and *A. niger, A. flavus* were studied using chlorompinacol and Fluconazole as a reference drugs, respectively. These bactericidal activities are less good than those of the standard drug used for comparison purposes.

From the antimicrobial screening results, it was seen that the H_2bnp is moderately active against bacteria, *E. coli, X. vesicatoria* and fungi, *A. niger* and *A. flavus*,. All the complexes have shown good activity against both bacteria and fungi. The activity of the ligand as well as that of metal salts has increased on complexation. Among the ligand and its complexes, the antifungal activity of complexes **1** and **2** is found to be greater but less than that of the fluconazole, the antifungal drug in use. The antibacterial activity of the synthesized compounds and standard are in the following order chloramphenicol > **1** > **2** > **3** > **4** > H_2bnp, while for antifungal activity order follows as fluconazole > **1** > **2** > **3** > **4** > H_2bnp. This result reflects the extent interaction of diimine ligand complex with the DNA.

The biological activity of the H_2bnp is considered to be related to its ability to form chelates with metals. On chelation, the polarity of the metal ion will be reduced to a greater extent due to the overlap of the ligand orbital and partial sharing of the positive charge of the metal ion with donor groups [51]. Furthermore, the mode of action of the compound may involve formation of a hydrogen bond through the azomethine group with the active centre of cell constituents, resulting in interference with normal cell processes.

4. Conclusions

The present study leads us to conclude that the complexes bind to CT DNA through their di-imine moiety strongly and that the nature of the di-imine - planarity dictates both their structure and DNA binding affinity. Thus, when the di-imine is phen the partial intercalative interaction of the complexes to DNA base pairs is facilitated leading to enhancement in DNA-binding affinity. The observations of the result obtained from the oxidative cleavage, set off the DNA damage and block DNA synthesis indirectly through inhibition of biosynthesis of precursor molecules for nucleic acids and make them better candidates for development as metallo-drugs. It is believed that the information obtained from the present work would ultimately be helpful to develop new potent antioxidants and new therapeutic agents for some diseases.

Acknowledgement

One of the authors H.D. Revanasiddappa is thankful to the University of Mysore for providing minor research project. The author L.S. Kumar is thankful to the University Grants Commission, New Delhi for the award of Rajiv Gandhi National Fellowship. We also thank Head of the Department of Biotechnology, for providing the help in carrying out antimicrobial and nuclease activities.

References

[1]. Thangadurai, T. D.; Natarajan, K. *Trans. Met. Chem.* **2002**, *27*, 485-489.
[2]. Frey, G. D.; Bell, Z. R.; Jeffery, J. C.; Ward, M. D. *Polyhedron* **2001**, *20*, 3231-3237.
[3]. Nath, M.; Pokharia, S.; Yadav, R. *Coord. Chem. Rev.* **2001**, *215*, 99-149.
[4]. El-Said, Al.; Zidan, A. S.; El-Meligy, M. S.; Aly, A. A. M. *Synth. React. Inorg. Met.-Org. Chem.* **2000**, *30*, 1373-1392.
[5]. Banerjee, S.; Mondal, S.; Chakraborty, W.; Sen, S.; Gachhui, R.; Butcher, R. J.; Alexandra M. Z. S.; Mandal, C.; Mitra S. *Polyhedron* **2009**, *28*, 2785-2793.
[6]. Abdel-Aziz, M.; Abdel-Rahman, H. M. *Eur. J. Med. Chem.* **2010**, *45*, 3384-3388.
[7]. Satyanarayana, V. S. V.; Sreevani, P.; Amaravadi, S.; Vijayakumar, V. *Arkivoc* **2008**, *17*, 221-233.
[8]. Singh, P. V.; Gupta. P. *J. Coord. Chem.* **2008**, *61*, 3922-3933.
[9]. Luo, W.; Meng, X. G.; Cheng, G. Z.; Ji. Z. P. *Inorg. Chim. Acta* **2009**, *362*, 551-555.
[10]. Li, Z.; Yang, Q.; Qian, X. *Bioorg. Med. Chem.* **2005**, *13*, 3149-3155.
[11]. Ranford, J. D.; Sadler, P. J; Tocher, D. A. *Dalton Trans.* **1993**, *22*, 3393-3399.
[12]. Maheswari, P. U; Roy, S.; Dulk. H. D.; Barends, S.; Wezel, G. V.; Kozlevcar, B.; Gamez, P.; Reedijk, J. *J. Am. Chem. Soc.* **2006**, *128*, 710-711.
[13]. Zelenko, O.; Gallagher, J.; Sigman, D. S. *Angew. Chem. Int. Ed. Engl.* **1997**, *36*, 2776- 2778.
[14]. Patel, M. N.; Chhasatia, M. R.; Gandhi, D. S. *Bioorg. Med. Chem. Lett.* **2009**, *19*, 2870-2873.
[15]. Selvakumar, B.; Rajendiran, V.; Maheswari, P. U.; Evans, H. S.; Palaniandavar, M. *J. Inorg. Biochem.* **2006,** *100*, 316-330.
[16]. Kourounakis, A. P.; Galanakis, D.; Tsiakitzis, K. *Drug. Dev. Res.* **1999**, *47*, 9-16.
[17]. Buyukokuroglu, M. E.; Gulcin, I.; Oktay M.; Kufrevioglu, O. I. *Pharm. Res.* **2001**, *44*, 491- 494.
[18]. Bravo-Gómez, M. E.; García-Ramos J. C.; Gracia-Mora, I.; Ruiz-Azuara, L. *J. Inorg. Biochem.* **2009**, *103*, 299-309.
[19]. Bukhari, B. S.; Memon, S.; Tahir, M. M.; Bhanger, M. I. *J. Mol. Struc.* **2008**, *892*, 39-46.
[20]. Bravo-Gomez, M. E.; García-Ramos, J. C.; Gracia-Mora, I.; Ruiz-Azuara, L. *J. Inorg. Biochem.* **2009**, *103*, 299-309.
[21]. Perrin, D. D.; Armarego, W. L. F.; Perrin, D. R. *Purification of Laboratory Chemicals*; Pergamon Press: Oxford, U. K., 1980.
[22]. Hassan, H. M.; Rahman, B.; Peter, M. *Acta Cryst.* **2010**, E66, o236-o237.
[23]. Satyanarayana, S.; Dabrowiak, J. C.; Chaires, J. B. *Biochemistry* **1993**, *32*, 2573-2584.
[24]. Banerjee, S.; Mondal, S.; Chakraborthy, W.; Sen, S.; Gachhui, R.; Butcher, R. J.; Slawin, A. M. Z.; Mandal, C.; Mitra, S. *Polyhedron* **2009**, *28*, 2785-2793.
[25]. Anbu, S.; Kandaswamy, M.; Suthakaran, P.; Murugan, V.; Varghese, B. *J. Inorg. Biochem.* **2009**, *103*, 401-410.
[26]. Blois, M. S. *Nature* **1958**, *26*, 1199-1200.
[27]. Ruch, R. J.; Cheng, S. J.; Klaunig, J. E. *Carcinogenesis* **1989**, *10*, 1003-1008.
[28]. Suffredini, J. B.; Sader, H. S.; Goncalves, A. G.; Reis, A. O.; Gales, A. C.; Varella, A. D.; Younes, R. N. *Brazil. J. Med. Biol. Res.* **2004**, *37*, 379-384.
[29]. Valko, M.; Boca, R.; Klement, R.; Kozisek, J.; Mazur, M.; Pelikan, P.; Morris, H.; Elias, H.; Muller, L. *Polyhedron* **1997**, *16*, 903-908.
[30]. Sathisha, M. P.; Shetti, U. N.; Revankar, V. K.; Pai, K. S. R. *Eur. J. Med. Chem.* **2008**, *43*, 2338-2346.
[31]. Yaul, S. R.; Yaul, A. R.; Pethe G. B.; Aswar, A. S. *Amer.-Eurasian J. Sci. Res.* **2009**, *4*, 229-234.
[32]. Ibrahim, Y.; Aladdin C. *Trans. Metal Chem.* **2003**, *28*, 399-404.
[33]. Lee, P. E.; Yong, C. T.; Fon, D.; Vittal, J. J.; Ranford, J. D. *Polyhedron* **2003**, *22*, 2781- 2786.
[34]. Andersen, K. B.; Spanget-Larsen, J. *Spectrochim. Acta Part A* **1997**, *53*, 2615-2625.
[35]. Brumas, V.; Miche, H.; Fiallo, M. *J. Inorg. Biochem.* **2007**, *101*, 565-577.
[36]. Ghosh, K.; Pramod, K.; Nidhi, T.; Singh, U. P.; Aggarwal, V.; Baratto, M. C. *Eur. J. Med. Chem.* **2010**, *45*, 3770-3779.
[37]. El-Wahab, Z. H. A.; Mashaly, M. M.; Faheim, A. A. *Chem. Paper* **2005**, *59*, 25-36.
[38]. Al-Hazmi, G. A.; El-Asmy, A. A. *J. Coord. Chem.* **2009**, *62*, 337-345.
[39]. Agarwal, R. K.; Deepak, S.; Singh, L.; Agarwal, H. *Bioinorganic Chem. Appl.* **2006**, *2006*, 1-9.
[40]. Mishra, A. P.; Soni, M. *Metal-Based Drugs* **2008**, *2008*, 1-7**.**
[41]. Ramakrishnan, S.; Palaniandavar M. *J. Chem. Sci.* **2005**, *117*, 179-186.
[42]. Surendra Babu, M. S.; Reddy, K. H.; Krishna, P. G. *Polyhedron* **2007**, *26*, 572-580.
[43]. Lepecq, J. B.; Paoletti, C. *J. Mol. Biol.* **1967**, *27*, 87-106.
[44]. Liu, J.; Zhang, T.; Lu, T.; Qu, L.; Zhou, H.; Zhang, Q.; Ji, L. *J. Inorg. Biochem*. **2002**, *91*, 269-276.
[45]. Lipscomb, L. A.; Zhou, F. X.; Presnell, S. R.; Woo, R. J.; Peek, M. E.; Plaskon, R. R.; Williams, L. D. *Biochemistry* **1983**, *35*, 2818-2823.
[46]. Chen, J.; Wang, X.; Shao, Y.; Zhu, J.; Zhu, Y.; Li, Y.; Xu, Q.; Guo, Z. *Inorg. Chem.* **2007**, *46*, 3306-3312.
[47]. Lakowicz, J. R.; Webber, G. *Biochemistry* **1973**, *12*, 4161-4170.
[48]. Stefan, B.; Susanne, F.; Hansgeorg, E.; Thomas, H.; Ines, H. B.; Claas, H.; Nicole, K.; Sebastian, K.; Hans-Dieter, M.; Bernhard, M.; Peter, N.; Perez-Galvez.; Antonio, G. K.; Roger, S.; Wolfgang, S.; Stefan, S.; Wilhelm, S. *Arkivoc* **2007**, *8*, 279-295.
[49]. Fatimah, Z. I.; Zaiton, Z.; Jamaludin, M.; Gapor, M. T.; Nafeeza, M. I.; Khairul, O.; Packer, S. H. Ong (Eds.), Biological Oxidants and Antioxidants: Molecular Mechanism and Health Effects, Illinois, AOCS Press, Champaign, 1998 Chapter 22.
[50]. Aruoma, O.; Kaur, H.; Halliwell, H. *J. Royal. Soc. Health* **1991**, *111*, 172-77.
[51]. Wang, Q.; Zheng-Yin, Y.; Gao-Fei, Q.; Dong-Dong, Q. *Biometals* **2009**, *22*, 927-940.